Spatial Dependence of Physical Properties of a Typic Torrifluvent Soil[1]

Y. M. GAJEM, A. W. WARRICK, AND D. E. MYERS[2]

ABSTRACT

The spatial structure of soil properties has been examined on a Typic Torrifluvent soil at The University of Arizona Experiment Station at Marana. Nine hundred samples from nine transects were collected in straight lines (100 locations for each transect), at 20-, 200-, and 2,000-cm intervals. All samples were at a 50-cm depth. Variables include 0.1 and 15 bar water content, available water, surface area, particle size distribution, pH, EC, bulk density, and moisture content in the field seven days after irrigation. Autocorrelation functions were evaluated for each parameter and found to be correlated over space with patterns of three basic types: typical, random, or with a large zone of influence. Generalizations were difficult, but the calculated zone of influence was strongly dependent on distance between samples, with larger intervals tending to give greater values. In a few cases, this could partially be explained on the basis of larger standard deviations measured on longer transects. Results indicate future difficulty in assigning scale lengths by parameter or soil.

Additional Index Words: **geostatistics, soil variability, autocorrelation.**

Gajem, Y. M., A. W. Warrick, and D. E. Myers. 1981. Spatial structure of physical properties of a Typic Torrifluvent soil. Soil Sci. Soc. Am. J. 45:709–715.

ONLY RECENTLY has interdependence of sites within sampling units been examined to any extent for soil physical properties. Infiltration and water movement were studied in the field by Sisson (1981), Vieira,[3] and Rogowski (1980). The latter two included calculations of sample semivariograms and punctual kriging for contouring and preparing variance maps. Kriging was also applied by Hajrasuliha et al. (1980) for water table heights and salinity on three large fields (150, 440, and 445 hectares) in southwestern Iran. Autocorrelograms were determined by Russo and Bresler (1981) for six measured parameters, including saturated hydraulic conductivity on four depths and 30 locations in a 0.8-ha field. Simulations for water and salt dispersion as stochastic, autocorrelated systems have been carried out by Smith and Freeze (1979) and Smith and Schwartz (1980). Studies such as these join other work (Webster, 1977; Campbell, 1978; Burgess and Webster, 1980a, b, c) which relate more to mapping and classification.

The objective of this study is to examine spatial structure of selected physical properties of the Pima clay loam, a Typic Torrifluvent. The experiment was designed in order to evaluate whether samples were interdependent and, if so, over what distance did this occur. Due to scarcity of previous information, we chose quite different spacings (20, 200, and 2,000 cm). Also, we chose a variety of relatively easily measurable parameters in order to maximize scope of the project while optimizing labor and precision. Only 1 depth (50 cm) was sampled in order to emphasize sampling and measurements areally. The number of samples (100) in each transect was taken so as to give an adequate series for comparison; the number of transects (nine) gives some replications and allows at least two different orientations.

SAMPLING AND MEASUREMENTS

In June 1979, nine transects were sampled as shown in Fig. 1 with 100 samples in each. Four transects were sampled at a 20-cm interval, four at 200 cm, and one at 2,000 cm, each in the direction of the arrow. The 2,000-cm transect went across the 85-ha University of Arizona farm and continued across the adjacent grower's field. The 85 ha shown in Fig. 1 is approximately 93% Pima clay loam (fine silty, mixed thermic family of Typic Torrifluvents). The sites shown are in areas previously mapped as Pima (Post et al., 1978).

Each 20-cm transect is on a common axis with one 200-cm transect which together have 10 points in common. For example, Transect 1–20 and Transect 1–200 are along the same north–south line. The sampling for Transects 1–20, 1–200, 2–20, and 2–200 were each in a growing cotton field, paralleling cotton rows at a 10-cm distance. Transects 3–20, 3–200, 4–20, and 4–200 were in a bare field, about 7 days after a heavy irrigation. The irrigation was by furrows, spaced 103-cm apart with

[1] Arizona Agric. Exp. Stn., Paper no. 3368. Supported by Western Regional Project W-155. Received 8 Oct. 1980. Approved 30 March 1981.

[2] Graduate Student, Dep. of Soils, Water, and Engr.; Professor, Dep. of Soils, Water, and Engr.; and Professor, Dep. of Math. Address: University of Arizona, Tucson, AZ 85721.

[3] S. R. Vieira. 1980. Spatial variability of field-measured infiltration rates. M.S. Thesis. Univ. of California, Davis.

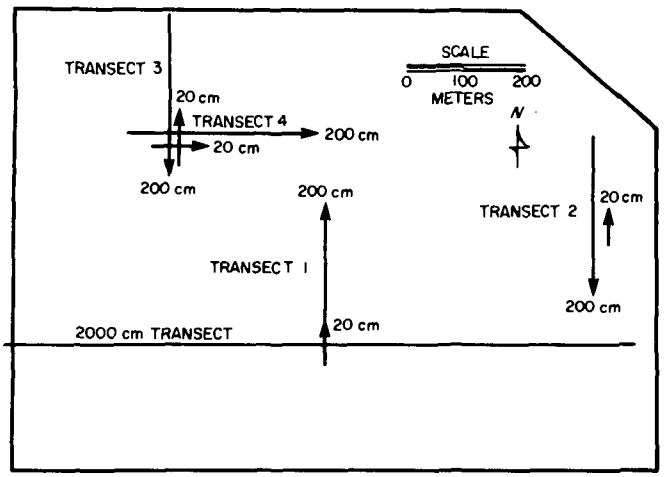

Fig. 1—Locations of the nine transects used at The Univ. of Arizona Exp. Stn. at Marana. Arrows indicate direction samples were collected. Total area is about 85 ha.

the water running south to north. Transects 3–20 and 4–20 crossed each other at right angles in the exact middle with no common points. Transects 3–200 and 4–200 also crossed at right angles with 15 sites to the south, 85 to the north, 30 to the west, and 70 to the east.

Bulk samples were collected in June 1979 with 7.6-cm bucket augers by collecting all of the soil between the 40- and 60-cm depth. The lower depth corresponds approximately to the average depth of the surface horizon (Post et al., 1978). Each transect was collected on the same day along consecutive locations. All sampling was within a 2-week period. The samples were air-dried, passed through a mechanical soil grinder, through a 2-mm sieve, and finally stored in plastic bags for analysis. In addition, samples were collected with a 2.5-cm diam probe at the same depth for Transects 3–20 and 3–200. These were carefully extracted and sealed in order to obtain moisture content and bulk density values.

Water retained at 0.1 and 15 bar water, soil pH on a 1:5 soil-to-water suspension, and electrical conductivity on a 1:5 extract were found on all 900 samples by standard techniques. Randomization of the order of determination was impractical, due to a large number of samples. Precision of measurements, however, was carefully checked and rechecked, and there was no evidence of systematic concentration of error. Table 1 shows estimated precision of measurement expressed as standard deviation (SD) and coefficient of variations (C.V.) for measurements on 4 to 6 split samples each. These were representative subsamples of the actual sites. Errors in the laboratory measurement will be discussed later relative to the transect variability.

Particle size and surface area were also determined on all 900 samples using the "Microtrac" (Leeds Northrup Model 7991-0, Southwest Rangeland Research Center, Tucson). The Microtrac analyzer uses a small angle, forward light scattering of a laser beam to measure soil particles with a diameter ranging from 2 to 176 μm. The distribution is expressed in 13 histogram channels, partitioning the fine and very-fine sand into four of these segments and the silt into the other nine. The microcomputer prints a number of parameters, including the volume mean diameter in microns and the specific surface of the sample. The specific surface value is given as m^2/cm^3 and is not identical to the physical surface area measured by polar retention. For preparation, about 4 g of dry soil were wet-sieved through a 180-μm sieve. One milliliter of a mixture of Na-pyrophosphate (53.5 g/liter) and Na-carbonate (4.24 g/liter) were added to each gram of soil as a dispersing agent. The soil suspension was dispersed by an ultrasonic mixer (Sonifier Cell Disruptor Model 350) for 2 minutes. After that, the soil suspension was transferred to the microtrac, and the results displayed on a LED (light emitting diode) readout. A digital printer recorded the data. A major advantage of the system is ease of measurement with reasonably repeatable values. For Transects 3–20, the particle size analysis was also determined by a standard hydrometer (152H — 20°C). Estimated precisions for both microtrac and hydrometer measurement are in Table 1.

Sample means and standard deviations are given for all

Table 1—Summary of precision of determinations.

Parameter†	No. subsamples in trial		Sample 1	Sample 2
0.1 bar	6	Mean	35.82	34.36
		SD	0.40	0.47
		C.V.	1.30	1.40
15 bar	6	Mean	12.50	11.80
		SD	0.90	0.80
		C.V.	7.20	6.80
Surface area (microtrac)	6	Mean	0.558	0.902
		SD	0.032	0.030
		C.V.	5.73	3.330
Mean diameter (microtrac)	6	Mean	57.4	30.1
		SD	3.90	3.36
		C.V.	6.80	11.2
pH (1:5 soil/water suspension)	5	Mean	8.70	–
		SD	0.05	
		C.V.	0.50	
EC (1:5 soil/water extract)	5	Mean	273.0	–
		SD	4.5	
		C.V.	1.6	
% Clay	4	Mean	34.7	32.8
		SD	1.3	1.1
		C.V.	3.8	3.5
% Silt	4	Mean	37.0	54.45
		SD	0.4	0.80
		C.V.	1.0	1.50
% Sand	4	Mean	28.3	12.75
		SD	1.3	0.50
		C.V.	4.6	3.90

† 0.1 bar and 15 bar water are expressed as percent gravimetrically. Surface area, mean diameter, and EC are m^2/cm^3, μm and μmho/cm, respectively.

transect parameter combinations in Table 2. The raw data is recorded by Gajem.[4] The "available water", loosely defined as water stored between the 0.1 and 15 bar water, is added for interest. The lowest C.V. values found were 1.1 to 2.3% for pH, and largest values of 41.2% for mean diam. In general, smaller values of C.V. corresponded to the short transects and larger values for longer transects.

STATIONARITY AND AUTOCORRELATION FUNCTIONS

We expect the values of a soil parameter at locations close together will be approximately the same or at least related, whereas when two locations are far apart, we expect the values to be unrelated. This change from strong dependence to independence can be quantitatively represented by the autocorrelation function of a random function.

The use of the autocorrelation function implies certain mathematical hypotheses, in particular a form of stationarity. In general, if the value of a parameter at a location p is represented by a random function $X(p)$, then the random function is STATIONARY if for any m points $p_1, \ldots, p_m$ the joint distribution of $X(p_1), \ldots, X(p_m)$ is invariant with respect to translations; that is, the distribution of $X(p_1+h), \ldots, X(p_m+h)$ is the same for all h. One consequence of stationarity is that if $X(p)$ also has finite mean μ and variance σ^2, then these do not depend on p. Moreover, the covariance of $X(p)$, $X(p+h)$ depends only on h. For the autocorrelation function we need only these latter properties since it is defined by

$$\rho(h) = \mathrm{Cov}\,[X(p), X(p+h)]/\sigma^2. \qquad [1]$$

[4] Y. M. Gajem. 1980. Spatial structure of physical properties of a Typic Torrifluvent. M.S. Thesis. Univ. of Arizona, Tucson.

Table 2—Mean, standard deviation, zone of influence, and type of correlogram for all transects and parameters.

Parameter	Mean	SD	Zone of influence, cm	Type of correlogram
	Transect 1-20 cm, C-2			
0.1 bar†	34.9	2.8	350	A
15 bar†	18.3	2.1	170	A
Available water†	16.7	3.1	>400	C
pH	8.9	0.1	160	A
EC†	223.0	27.9	0	B
Surface area†	1.1	0.1	140	A
Mean diameter†	13.8	2.2	120	A
	Transect 2-20 cm, E-3			
0.1 bar	21.0	1.2	100	Indefinite
15 bar	8.2	1.1	60	Indefinite
Available water	12.8	1.4	20	B
Surface area	0.67	0.05	60	A
Mean diameter	51.4	4.1	80	A
pH	8.8	0.1	120	Indefinite
EC	136.0	11.6	120	Indefinite
	Transect 3-30 cm, B-4			
0.1 bar	36.7	1.6	60	B
15 bar	21.1	1.4	0	B
Available water	15.6	1.6	20	B
Surface area	1.01	0.08	160	Indefinite
Mean diameter	20.6	4.9	400	C
pH	8.2	0.2	260	A
EC	350.0	74.2	300	A
Bulk density	1.38	0.2	340	A
Moisture content	14.7	2.4	240	A
Clay %	31.8	5.2	>500	C
Silt %	50.9	9.4	>500	C
Sand %	17.3	5.5	>500	C
	Transect 4-20 cm, B-4			
0.1 bar	37.0	1.9	0	B
15 bar	17.9	1.5	0	Indefinite
Available water	19.1	1.7	0	Indefinite
Surface area	0.88	0.06	0	Indefinite
Mean diameter	23.1	3.8	0	Indefinite
pH	8.7	0.11	40	B
EC	186.0	20.9	40	A
	Transect 1-200 cm, C-2			
0.1 bar	35.3	2.9	1,000	Indefinite
15 bar	19.3	2.5	4,000	C
Available water	16.0	2.4	200	Indefinite
Surface area	1.05	0.07	400	A
Mean diameter	15.4	3.0	0	B
pH	8.8	0.1	1,200	A
EC	212.0	30.3	1,600	Indefinite
	Transect 2-200 cm, E-3			
0.1 bar	29.4	4.4	4,000	C
15 bar	13.3	3.0	3,600	A
Available water	16.1	1.9	3,400	C
Surface area	0.83	0.13	2,800	A
Mean diameter	36.80	11.0	2,600	A
pH	8.6	0.1	1,400	A
EC	161.0	23.4	>4,000	C
	Transect 3-200 cm, B-4			
0.1 bar	34.2	3.6	>4,600	C
15 bar	19.0	2.7	1,400	A
Available water	15.1	2.4	>4,600	C
Surface area	0.96	0.11	800	A
Mean diameter	25.2	10.4	>4,600	C
pH	8.4	0.12	2,800	A
EC	234.0	33.8	1,800	A
Bulk density	1.25	0.1	200	B
Moisture content	20.7	4.9	>4,600	C
	Transect 4-200 cm, B-4			
0.1 bar	34.0	3.6	>4,000	C
15 bar	18.4	3.0	>4,000	C
Available water	15.5	2.1	0	Indefinite
Surface area	0.89	0.07	200	B
Mean diameter	29.10	6.5	600	A
pH	8.5	0.14	3,200	A
EC	162.0	16.3	600	indefinite
	Transect 2,000-cm intervals, field			
0.1 bar	32.6	6.7	16,000	A
15 bar	14.1	4.3	15,000	A
Available water	18.5	3.74	12,000	A
Surface area	0.92	0.2	28,000	A
Mean diameter	26.3	10.5	26,000	A
pH	8.8	0.12	13,000	A
EC	176.0	53.4	2,000	B

† 0.1, 15 bar, available water, and moisture content are expressed as percent gravimetrically. Surface area, mean diameter, EC, and bulk density are m^2/cm^3, μm, $\mu mho/cm$, and g/cm^3, respectively.

If the joint distributions were known, then $\rho(h)$ could be computed directly, but of course it almost never is and instead $\rho(h)$ will have to be estimated from the data using the sample autocorrelation function. In using the autocorrelation function we should remember that we are modelling the soil parameter by a random function with sufficient properties to ensure the existence of the autocorrelation function. The validity of these assumptions generally cannot be tested satisfactorily and may depend on the area or volume of the region modelled. Stationarity in particular is often a matter of scale, both of the region and also the sampling intervals.

The vector h can have both direction and length, but for simplicity of analysis, we have considered only samples along a transect, i.e., h has only magnitude. Since the sampling was regular, it is possible to count "lags" instead of measuring distances; this has advantages and disadvantages. Since the number of sample locations was the same irrespective of the distance betwen them, for example, using lags would enhance any invariance with respect to change of scale. On the other hand, if we wish to determine a zone of influence in absolute terms, the use of lags could obscure it. To provide some information about the effect of a directional component for h, we have included both N–S and E–W transects.

In a subsequent section we will describe the use of another quantitative characterization of spatial dependence, namely semivariograms. The autocorrelation function has certain advantages even though it requires a relatively strong form of stationarity. In particular, the values of the autocorrelation function are normalized to the range −1,1 inclusive; this makes it easier to interpret the values. Fourier analysis is a well-known tool for analyzing $\rho(h)$ and can be useful. Finally, in the case where the random function is jointly normal or jointly log-normal, it is only necessary to know the mean, variance, and $\rho(h)$ to completely characterize the random function.

As noted before, we have to use the sample autocorrelation function $r(h)$ to estimate $\rho(h)$. There are several formulas in use for $r(h)$, we have followed that in Agterberg (1974). Since the sampling was on regular intervals, we can simplify the notation by letting $X(p_i) = X_i$. Note that s^2 is not an unbiased estimator of σ^2 because of the dependence. The sample covariance C_k is given by

$$C_k = 1/(n-k+1) \sum_{i=1}^{n-k+1} (X_{i+k}-\bar{X})(X_i-\bar{X}), \quad [2]a$$

$$C_o = s^2, \quad [2]b$$

where $\bar{X}$ is the sample mean. The sample autocorrelation function then is given by

$$r_k = C_k/s^2, \quad [3]$$

where k is the number of lags and n is the number of sample locations.

It would seem that $\rho(h)$ would be an intrinsic characteristic of the soil parameter, but this is not quite so since it is instead a characteristic of the random function used to model the parameter which may depend on the size of the region and mathematical assumptions. This dependency is very likely true of the sample autocorrelation function, even more than for $\rho(h)$.

In this paper we have described the types of autocorrelation functions observed for various soil parameters in Pima clay loam, and we have determined zones of influence as inferred from the autocorrelograms.

Autocorrelograms

The autocorrelogram is a plot of r_k as a function of distance or the lag k. The maximum value is 1 at 0 lag ($k = 0$) and the values tend to decrease with increasing k. When $k = 1$ and points 1, 2, . . . , n are evenly spaced, we correlate X_1 with X_2, X_2 with X_3, . . . , X_{n-1} with X_n. For $k = 2$, we correlate X_1 with X_3, X_2 with X_4, . . . , X_{n-2} with X_n.

Three types of correlograms are shown in Fig. 2, the first (*A*) is a fairly typical case with the value of r_k dropping gradually to 0 and leveling off. In the next case (*B*), the value drops to 0 much sooner, in fact within 1 lag. Thus, in (*B*) the samples are not correlated, but are independent of each other. In (*C*), the correlogram drops off from 1 but much slower, indicating a dependence over a long range. Other possibilities include cyclic patterns and nested structures which are not shown here.

The 0.1 bar moisture content values for Transect 1-20 (Transect 1, 20-cm spacing) are shown as Fig. 3A. Values ranged from 29 to 43% with an experimental mean and standard deviation of 35 and 2.8, respectively. Values tend to be higher at the left, decrease toward the middle, and increase again at the right. The corresponding autocorrelogram is given as Fig. 3B. The plot of r_k is somewhat similar to Fig. 2A with values > 0.2 out as far as 20 lags (400 cm). The immediate drop to 0.5 at 1 lag could correspond to a "nuggest effect" (Journel and Huijbregts, 1978).

A question naturally arises as to what is the "zone of influence" beyond which values are independent of each other. Examining Fig. 3B, we observe r_k drops off to negligible values. One procedure to test the hypothesis that the population autocorrelation $|\rho_k|$ is 0 is by using the statistic Z_k (Davis, 1973):

$$Z_k = |r_k| \sqrt{n-k}, \quad [4]$$

with n the length of the sequence, and k the lag. The value for Z_k is calculated and compared to the tabulated two-tailed deviation Z_α^*. If $Z_k > Z_\alpha^*$, we reject the hypothesis and accept the alternative that $|\rho_k|$ is > 0. We can solve for a zone of influence (ZI) by setting $Z_k = Z_\alpha^*$ in Eq. [4], solving for k and converting from lags to distance:

$$\text{ZI/(Spacing)} = k^* = n - (Z_\alpha^*/r_k^*)^2, \quad [5]$$

where k^* and r_k^* are the number of lags and value of the autocorrelation coefficient at ZI. If we choose $\alpha = 0.05$, we find $Z_{.05} = 1.645$. For the smoothed curve through Fig. 3B, we find ZI = 350 cm.

For bulk density and moisture content in the field 7 days after irrigation, the results are examined in Fig. 4 for the 3-20 and 3-200 transects. The bulk density and the moisture content results for the 3-20 transect are correlated in the same manner as the example given in Fig. 3B and is similar to that in Fig. 2A. The bulk density results for the 3-200 transect indicate a random pattern similar to Fig. 2B. The moisture content results for the 3-200 transect are considerably above 0 even at 23 lags, indicative of long correlation similar to that presented in Fig. 2C.

These appear to be easily explainable. The ZI for the bulk density is about 340 cm for the short spacing and is hardly discernible (20 cm is only 1 lag) for the larger 200 cm spacing. This would indicate a short range of influence, detectable only using the short spacing. The short transect gives a similar range (240 cm) for the moisture content. However, we find a much larger value (> 4600 cm) for the 200-cm water content. This large value can be rationalized by ob-

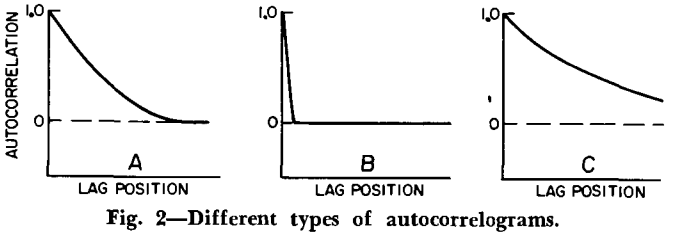

Fig. 2—Different types of autocorrelograms.

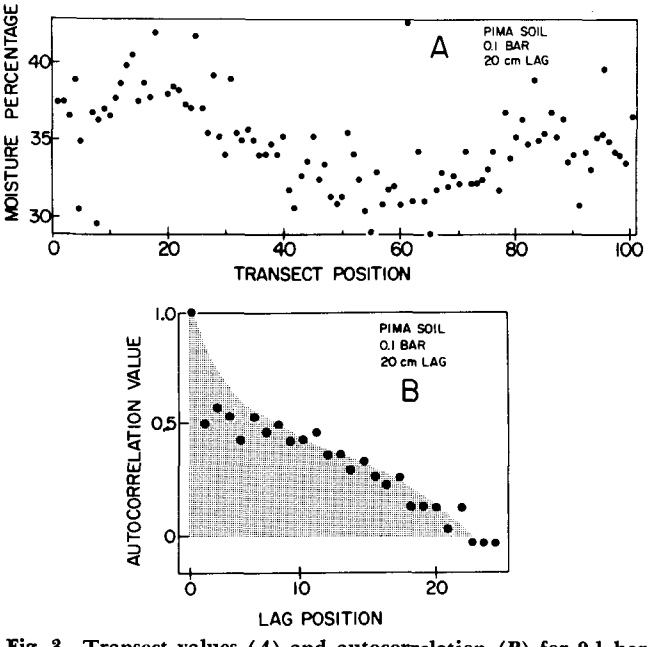

Fig. 3—Transect values (*A*) and autocorrelation (*B*) for 0.1 bar water of Pima clay loam. Shaded area was used to estimate integral scale of Eq. [6]a.

serving that the irrigation was from south to north. The slope was such that more water infiltrated at the head of the furrow (the original data is in Gajem[4]). The sample standard deviations, 4.9 for the long spacing and 2.4 for the short spacing, also are consistent.

Table 2 includes types of autocorrelation patterns and ZI values for all 70 parameter-transect combinations. Of the 70 autocorrelelograms (all 70 are plotted in Gajem[4]), 30 were judged of Type A (of Fig. 2), 11 of Type B, 15 of Type C, and 14 were "indefinite" (i.e., not clearly A, B, or C). When the $|\rho_k|$ was estimated to be > 0 at the length of the last lag plotted, we simply denoted ZI as "greater than" that value.

Transect 4–20 would also seem explainable on the basis of management. This short transect was the only one going perpendicular to the rows. The furrows were on a standard spacing of 103 cm. Results show Transect 4–20 to be nearly random with a short range of influence in nearly every case, whereas the north–south Transect 3–20 has values up to 300 or 400 cm on some of the same parameters (i.e., surface area, mean diam, pH, and EC).

The rest of the values for zone of influence are much harder to explain and offer few clear patterns other than bigger values for the larger transects. Most of the parameters on the 20-cm transect have zones of influence in the 100- to 300-cm range. Most of the 200-cm transects show values in the 2,000 to 4,000 range, approximately the same number of lags. For all parameters, the long transect shows values between 20 to 160 m.

An alternative to the ZI are "integral scales" as used by Bakr et al. (1978):

$$\lambda = \int_0^\infty r(x)dx, \qquad [6]a$$

and Russo and Bresler (1981):

$$\lambda^* = \left[\int_0^\infty xr(x)dx\right]^{1/2} \qquad [6]b$$

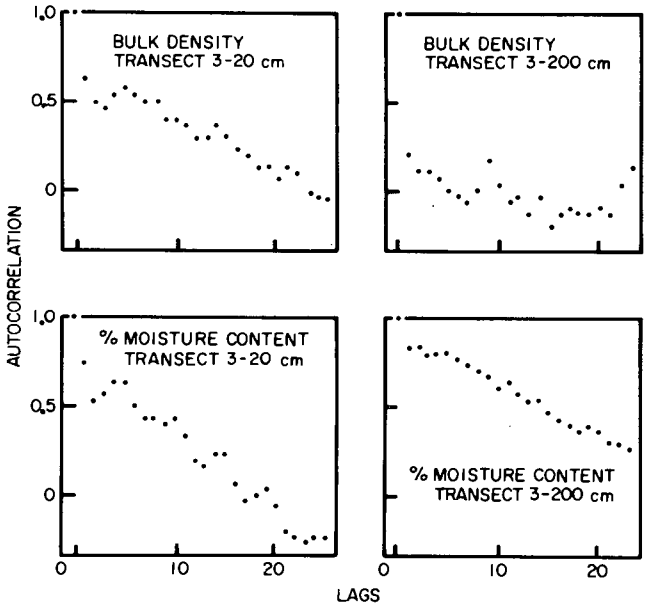

Fig. 4—Autocorrelation for bulk density and moisture content 7 days after irrigation at 20- and 200-cm intervals.

where r is the autocorrelation as a function of distance x. The integral scale for the 0.1 bar can be approximated by the shaded area of Fig. 3B. By using a planimeter the area and multiplying by the lag length, we find $\lambda = 160$ cm. Integral scales for all the combinations were found by Gajem[4]. The integral scales are smaller than the ZI and are related approximately as

$$ZI = (0.874)\ \lambda^{1.10}. \qquad [7]$$

Russo and Bresler (1981) found values of λ^* of 8 to 54 m for their 80- by 100-m plot. Vieira[3] found 35 m as the limiting range for infiltration on his site; Campbell (1978) found limiting ranges of 30 and 40 m for percent sand in two soils and random variation for pH.

Semivariograms

Although the autocorrelation function is useful for prediction/estimation of time series using Fourier analysis, there are analytic difficulties in two dimensions, and stationary in a moderately strong form is necessary. The technique known as kriging relaxes some of those conditions and computationally is somewhat simpler. Developed originally by G. Matheron and his associates for estimating ore grades in a mine, it has subsequently been applied to a wide range of problems (for a complete presentation of the basic ideas, see Journel and Huijbregts, 1978). More recently, Burgess and Webster (1980a, b, c) have used kriging to produce isarithmic soil maps. In this report we have only provided comparisons between the use of autocorrelation functions and semivariograms to quantify spatial variability. We will report on the use of kriging subsequently.

The principal tool in the use of kriging is the semivariogram function defined by

$$\gamma(h) = (1/2)\mathrm{Var}[Z(x) - Z(x+h)], \qquad [8]$$

where $Z(x)$ is a random function representing the soil parameter in question at location x, and where $\gamma(h)$ is assumed to be a function of h alone. It is not necessary for $Z(x+h) - Z(x)$ to have finite variance implying that $Z(x+h) - Z(x)$ must have a finite mean. This mean is called the "drift" of $Z(x)$; it is not quite the same as "trend" in the terminology of Trend Surfaces. The simplest form of drift is no drift, i.e., the mean is zero. This is implied by stationarity of $Z(x)$ with finite mean. Under the zero drift assumption, $\gamma(h)$ has the simpler form

$$\gamma(h) = E[Z(x+h) - Z(x)]^2. \qquad [9]$$

It is in this form that the semivariogram is most commonly used and most easily estimated from the data.

When the random function is stationary with finite variance, $\gamma(h)$ and $\rho(h)$ are related by the expression

$$\gamma(h) = \sigma^2\ [1 - \rho(h)].$$

It is known that autocorrelation functions must be positive definite and hence have Fourier integral representations. In the stationary finite variance case then $-\gamma(h)$ would be positive definite but, more generally, it is only necessary that $-\gamma(h)$ be conditionally positive definite.

In comparing the range of values of the two kinds of functions, we note that, unlike $\rho(h)$, $\gamma(h)$ is not

Table 3—Average value of standard deviation, precision, and zone of influence.

Parameter	20-cm Spacing			200-cm Spacing			2,000-cm Spacing		
	SD	Relative precision	Zone of influence	SD	Relative precision	Zone of influence	SD	Relative precision	Zone of influence
0.1 bar water	1.88	94	128	3.63	98	>3,400	6.70	99	16,000
15 bar water	1.53	69	58	2,80	91	>3,250	4.30	96	15,000
Surface area	0.07	80	90	0.10	90	1,050	0.20	98	28,000
Mean diameter	3.75	6	150	7.73	78	1,950	10.5	88	26,000
pH	0.13	85	145	0.12	83	2,150	0.12	83	13,000
EC	33.7	98	115	26.0	97	2,000	53.4	99	2,000
Bulk density	0.2	-	200	0.10	-	200	-	-	-
Moisture content	2.4	-	240	4.90	-	>4,600	-	-	-
Clay %	5.2	94	>500	-	-	-	-	-	-
Silt %	9.4	100	>500	-	-	-	-	-	-
Sand %	9.5	94	>500	-	-	-	-	-	-

normalized and has only non-negative values. In the case of stationarity from the relationship above we see that whereas $\rho(h)$ decreases as the magnitude of h increases, $\gamma(h)$ increases. If the variance of $Z(x)$ is finite and also bounded in the region, then $\gamma(h)$ will approach this value. Theoretically $\gamma(0) = 0$ but the sample semivariogram frequently exhibits a discontinuity or nonzero value there. There are several possible explanations for this behavior near $h = 0$. If there is a lack of data locations that are close together, it may appear to be non-zero for lack of sufficient information to extrapolate. It may also be caused by the presence of a white noise component in the random function. Krige observed this in analyzing data from gold fields and called it the "Nugget effect." In part it reflects the relationship between the size of the sample, i.e., the volume/length/area, and the intersampling distance.

Like the autocorrelation functions, $\gamma(h)$ must be estimated rather than computed. The usual estimator is the sample semivariogram given by

$$\gamma^*(h) = [1/N(h)] \Sigma\{Z(x) - Z(x+h)\}^2, \quad [10]$$

where the sum is for $N(h)$ terms, the number of points or locations "h" apart. Although this is an unbiased estimator it can be sensitive to the presence of outliers and a completely satisfactory estimator has not been found.

In the case where $\gamma(h)$ depends only on the magnitude of h and not on the direction, both $Z(x)$ and $\gamma(h)$ are called isotropic. The usual practice is to compute and plot sample semivariograms along transects in several directions and compare visually.

There are several important differences in the use of autocorrelation functions and semivariograms to characterize spatial variability. One of the most important is that the semivariogram can be used with weaker hypotheses, for example, nonfinite variance. This means that some parameters cannot be characterized by the autocorrelation function. With respect to stationarity, it might be possible to remove the nonstationary component with respect to either, but the semivariogram used in conjunction with kriging provides a convenient mechanism for doing so. While both the sample autocorrelation function and the sample semivariogram are affected by the area/volume of the sample at each location, the semivariogram provides the easiest mechanism for removing or identifying this effect. It is analogous to removing the "within block" variance in classical terms.

The sample semivariograms for bulk density and percent silt for Transect 3-20 are shown as Fig. 5. No drift was used in the analysis; the number of calculation lags was 70. For the bulk density value, the semivariogram increases and levels off to a value approximately equal to the variance (this corresponds to a correlogram of Type A, Fig. 2). On the other hand, the silt keeps increasing for the entire range (which corresponds to Type C of Fig. 2).

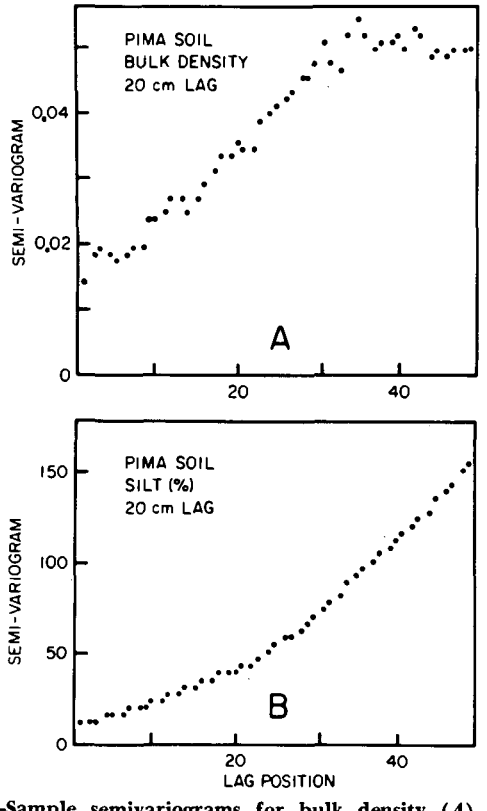

Fig. 5—Sample semivariograms for bulk density (*A*) and % silt (*B*), Transect 3-20.

SUMMARY AND CONCLUSIONS

The spatial variability and autocorrelation functions were studied for 11 physical parameters of a Typic Torrifluvent soil. The parameters were 0.1 and 15 bar water content, specific surface area, mean diam, pH, EC, bulk density, moisture content in the field 7 days after irrigation, and percent sand, silt, and clay. Four 20-cm interval transects along with four 200-cm transects and one 2,000-cm transect were chosen

for most of the first six parameters.

Table 3 summarizes values of the standard deviation and zone of influence for measured values. Both the standard deviations and zone of influence increase with spacing. In order to quantify the effect of field variation vs. the laboratory measuring error, we define a "relative precision" as

$$\text{relative precision} = [(s^2 - s_m^2)/s^2]\ (100\%),$$

where s_m^2 is a measurement variance as given in Table 1. If the laboratory measurement is without scatter, the relative precision is 100%. If the laboratory measuring error is large, the precision factor drops in relation to the overall variance measured in the field. The factor underscores the importance of knowing the measuring error. If the variance within split samples is large relative to the field variance, there is little need for studying variability for that property as the determination would be dominated by "white noise." The very low value for mean diameter reflects in part the fact that the precision was checked for a much larger diameter than the average value. Presumably, if precision had been tested in finer textures, the s_m^2 would have been smaller.

For the 20-cm spacing the range of zone of influence is 57.5 to > 500 cm with the lowest value for 15 bar water and highest value for percentage of sand, silt, and clay. For the 200-cm spacing, the range of zone of influence is 200 to > 4,600 cm, with the lowest value for bulk density and highest value for moisture content in the field. Such a range can only partially be explained on the basis of the larger variances. One possibility is lack of stationarity of the underlying system. There was also strong indications of non-isotropy in Transects 3 and 4–20 cm. In that case, the effects of the furrowing probably dominated over "natural" effects. The study would caution against overgeneralizing for results collected on one set of measured values while assuming the range of influence is unique.

The moisture content for Transects 3–20 and 3–200 is particularly interesting in that the measurements reflect the irrigation efficiency. For the 200-cm transect, the measured trend of south to north is more a function of how the water was added than soil variation. For the 20-cm spacing, the effects of watering are less important and the variation in soil more dominant (although uniformity in land preparation is still a factor).

LITERATURE CITED

1. Agterberg, F. P. 1974. Geomathematics. Elsevier, New York.
2. Bakr, A. A., L. W. Gelhar, A. L. Gutjahr, and J. R. MacMillan. 1978. Stochastic analysis of variability in subsurface flows: 1. Comparison of one- and three-dimensional flows. Water Resour. Res. 14:263–271.
3. Burgess, T. M., and R. Webster. 1980a. Optimal interpolation isarithmic mapping of soil properties: I. The semivariogram and punctual kriging. J. Soil Sci. 31:315–331.
4. Burgess, T. M., and R. Webster. 1980b. Optimal interpolation isarithmic mapping of soil properties: II. Block kriging. J. Soil Sci. 31:333–341.
5. Burgess, T. M., and R. Webster. 1980c. Optimal interpolation isarithmic mapping of soil properties: III. Changing drift and universal kriging. J. Soil Sci. 31:505–524.
6. Campbell, J. B. 1978. Spatial variation of sand content and pH within single continuous delineations of two mapping units. Soil Sci. Soc. Am. J. 42:460–464.
7. Davis, J. C. 1973. Statistics and data analysis in geology. John Wiley & Sons, Inc., New York.
8. Hajrasuliha, S., N. Baniabbassi, J. Matthey, and D. R. Nielsen. 1980. Spatial variability of soil sampling for salinity studies in southwest Iran. Irrigation Science 1:197–208.
9. Journel, A. G., and C. J. Huijbregts. 1978. Mining Geostatistics. Academic Press, New York.
10. Post, D. F., D. M. Hendricks, and O. J. Pereira. 1978. Soils of the university experiment station: Marana. SWE Dep., Series 78-1. The Univ. of Arizona, Tucson.
11. Rogowski, A. 1980. Hydrologic parameter distribution on a mine spoil. p. 764–780. Proc. of Symp. on Watershed Management. July 1980. Boise, Idaho. Am. Soc. Civil Engr., Boise, Id.
12. Russo, D., and E. Bresler. 1981. Soil hydraulic properties as stochastic processes: I. An analysis of field spatial variability. Soil Sci. Soc. Am. J. 45:682–687.
13. Sisson, James B., and P. J. Wierenga. 1981. Spatial variability of steady-state infiltration rates as a stochastic process. Soil Sci. Soc. Am. J. 45:699–704.
14. Smith, L., and R. A. Freeze. 1979. Stochastic analysis of steady-state ground water flow in a bounded domain: I. One-dimensional simulations. Water Resour. Res. 15(3): 521–528.
15. Smith, L., and F. W. Schwartz. 1980. Mass transport. A stochastic analysis of macroscopic dispersion. Water Resour. Res. 16:303–313.
16. Webster, R. A. 1977. Quantitative and numerical methods in soil classification and survey. Clarendon Press, Oxford.